Crystal structure and thermochemical properties of bis(1-octylammonium) tetrachlorochromate phase change materials*

Lu Dong-Fei(卢冬飞), Di You-Ying(邸友莹)†, and He Dong-Hua(何东华)

Shandong Provincial Key Laboratory of Chemical Energy Storage and Novel Cell Technology, College of Chemistry and Chemical Engineering, Liaocheng University, Liaocheng 252059, *China*

(Received 29 November 2011; revised manuscript received 20 February 2012)

A new crystalline complex $(C_8H_{17}NH_3)_2CdCl_4(s)$ (abbreviated as $C_8Cd(s)$) is synthesized by liquid phase reaction. The crystal structure and composition of the complex are determined by single crystal X-ray diffraction, chemical analysis, and elementary analysis. It is triclinic, the space group is P-1 and $Z = 2$. The lattice potential energy of the title complex is calculated to be U_{POT} ($C_8Cd(s)$)=978.83 kJ·mol^{-1} from crystallographic data. Low-temperature heat capacities of the complex are measured by using a precision automatic adiabatic calorimeter over a temperature range from 78 K to 384 K. The temperature, molar enthalpy, and entropy of the phase transition for the complex are determined to be 307.3±0.15 K, 10.15±0.23 kJ·mol^{-1}, and 33.05±0.78 J·K^{-1}·mol^{-1} respectively for the endothermic peak. Two polynomial equations of the heat capacities each as a function of temperature are fitted by using the least-square method. Smoothed heat capacity and thermodynamic functions of the complex are calculated based on the fitted polynomials.

Keywords: bis(1-octylammonium) tetrachlorochromate, X-ray crystallography, phase change materials, low-temperature heat capacity, solid–solid phase transition

PACS: 07.20.Mc, 61.50.Ks, 64.70.K–, 67.25.bd **DOI:** 10.1088/1674-1056/21/8/080702

1. Introduction

Phase change material (PCM) is also called a latent thermal energy storage material. It is an environmentally friendly material. It can be used as a low carbon building material for new city planning because of its zero discharge and pollution, which not only suits low carbon living, but also is good for the global climate. A variety of PCMs are available and well known for their thermochemical characteristics. These materials can be encapsulated by a polymer cover and currently exist in the market.[1] In recent decades, solid–solid phase change material (SSPCM) has become one of the most promising materials because of its excellent energy storage and release performances, such as little change in volume, no volatilization and shape plasticity, and so on.

As a kind of solid–solid phase change material, plenty of studies[2−8] of the complexes (n-$C_nH_{2n+1}NH_3)_2MX_4$ are reported, in which M is a divalent transition metal ion (M=Zn^{2+}, Cu^{2+}, Mn^{2+}, Cd^{2+}, Co^{2+}, etc.), X is a halogen, and n varies between 8 and 18. (n-$C_nH_{2n+1}NH_3)_2MX_4$ has many advantages. They can be applied conveniently in many fields such as solar energy utilization, temperature controlled greenhouses, peak load shifting technology, waste heat recovery, energy efficient air conditioning, and so on.[9,10] In the present article, we extend our investigation to the crystal structure and phase transition of ($C_8Cd(s)$), which needs to develop its new application fields and to be studied theoretically.

Adiabatic calorimetry is one of the most effective and important experimental methods used to measure the heat capacities of some important substances due to its high accuracy. And it can be widely used to study the solid–solid phase transitions by measuring low temperature heat capacities and calculating relevant thermodynamic data. Heat capacity is one of the most fundamental thermodynamic properties of a material and necessary for many theoretical studies in physics, chemistry, and engineering technology related to materials. Based on heat-capacity measurements, thermodynamic properties, such as the temperature, molar enthalpy, and entropy of the phase transition, and thermodynamic functions of the material can be

*Project supported by the National Natural Science Foundations of China (Grant Nos. 20673050 and 20973089).

†Corresponding author. E-mail: diyouying@126.com, diyouying@lcu.edu.cn

© 2012 Chinese Physical Society and IOP Publishing Ltd

precisely derived.[11−14]

In the present article, we synthesize a new crystalline complex ($C_8Cd(s)$) via liquid phase reaction. The crystal structure and composition of the complex are determined by using the X-ray single-crystal diffraction technique, chemical analysis, and element analysis. The lattice potential energy is obtained from crystallographic data. Low-temperature heat capacities of ($C_8Cd(s)$) are measured by using an accurate automatic adiabatic calorimeter in a temperature range from 78 K to 384 K and its thermodynamic properties are derived. The solid-to-solid phase transition is investigated analyzing the heat capacity curve of the complex ($C_8Cd(s)$).

2. Experiment

2.1. Synthesis of the title complex

The N-octylamine (purchased from J & K Scientific Ltd., China), hydrochloric acid (37% in mass percent), and hydrate cadmium chloride as reactants and anhydrous methyl alcohol as solvent are all of analytical grade. The reactants are accurately weighed at the molar ratio of $n(C_nH_{2n+1}NH_2)$: n(hydrochloric acid): $n(CdCl_2{\bullet}2.5H_2O)$ = 2:2:1, where hydrochloric acid is slightly excessive and slowly dissolved in anhydrous methyl alcohol. The mixture is heated by an electric jacket and stirred under boiling and refluxing for 4 h. The final solution is laid aside, and several days later, the colourless and transparent crystals are obtained. The crystals are recrystallized three times with anhydrous methyl alcohol and washed with ether three times. Finally, the sample is placed in a vacuum desiccator at T = 300 K to dry in vacuum for 6 h, the final product is put into a weighing bottle and preserved in a desiccator. Theoretical contents of C, H, N, Cd, and Cl in the complex $(C_8H_{17}NH_3)_2CdCl_4(s)$ are calculated to be 37.34%, 7.83%, 5.44%, 21.84%, and 27.55%, respectively. Chemical and elemental analyses (model: PE-2400, Perkin Elmer, USA) show that the practical content values of the C, H, N, Cd, and Cl in the complex $(C_8H_{17}NH_3)_2CdCl_4(s)$ are measured to be 37.36%, 7.86%, 5.40%, 21.82%, and 27.56%, respectively. These results show that the purities of the sample prepared are > 0.994 in mass fraction.

2.2. X-ray crystallography

X-ray crystallography is applied to characterize the crystal structure of the complex. The crystal is glued to a fine glass fiber and then mounted on the Bruker Smart-1000 CCD diffractometer with Mo–Kα radiation, λ = 0.71073 Å (1 Å=0.1 nm). The intensity data are collected in the φ–ω scan mode at T = 298(2) K. The empirical absorption corrections are based on multi-scanning. The structure is solved by using the direct method and different Fourier syntheses, and all non-hydrogen atoms are refined anisotropically on F^2 by using the full-matrix least-squares method. All calculations are performed with the program package SHELXTL.[15] We have applied for the CCDC number 855391 for the new compound $(C_8H_{17}NH_3)_2CdCl_4(s)$.

2.3. Adiabatic calorimetry

A precision automatic adiabatic calorimeter is used to measure the heat capacity of the complex over the temperature range 78 K$\leq T \leq$ 400 K. The calorimeter is established in the Thermochemistry Laboratory of the College of Chemistry and Chemical Engineering, Liaocheng University, China. The principle and performance of the adiabatic calorimeter and the procedures of heat capacity measurements have been described in detail elsewhere.[11,16] Heat-capacity measurements are continuously and automatically carried out using the standard method of intermittently heating the sample and alternately measuring the temperature. Liquid nitrogen is used as a coolant. The heating rate and temperature increments are generally controlled at 0.1 K·min^{-1} to 0.4 K·min^{-1} and 1 K to 3 K. The heating duration is 10 min, and the temperature drift rates of the sample cell measured in an equilibrium period are always kept within $\pm10^{-3}$ K·min^{-1} during the acquisition of all heat–capacity data. The data of heat capacities and corresponding equilibrium temperature are corrected for heat exchange of the sample cell with its surroundings.[16] The reliability of the performance of the calorimeter is confirmed by measuring the heat capacities of the reference standard material (α-Al_2O_3) over the temperature range 78 K$\leq T \leq$ 400 K. Deviations of the experimental results from those of the smoothed curves lie within $\pm$0.20%, while the uncertainty is $\pm$0.30% as compared with the values given by the former National Bureau of Standards[17] over the whole temperature range.

The sample mass used for calorimetric measurement is 1.96766 g for ($C_8Cd(s)$), which is equivalent to 3.8236×10^{-3} mol in terms of its molar mass, $M(C_8Cd(s))$ = 514.70 g·mol^{-1}.

3. Results and discussion

3.1. Description of crystal structure

The crystal data and details of data collection and refinements for the title complex are summarized in Table 1. The selected bond lengths and angles for the title complex are listed in Table 2, and the hydrogen bond lengths and angles are presented in Table 3. It is found from Table 1 that the crystal structure of the complex is triclinic, and the space group is P-1 and $Z = 2$. The molecular structure of ($C_8Cd(s)$) is plotted in Fig. 1. The packing of the cell structure is shown in Fig. 2.

Table 1. Crystal data and structure refinement for $C_8Cd(s)$.

Empirical formula	$(C_8H_{17}NH_3)_2CdCl_4$
Formula weight	514.70
Temperature/K	298(2)
Wavelength/Å	0.71073
Crystal system, space group	triclinic, P-1
Unit cell dimensions	$a = 7.4450(7)$ Å, $\alpha = 96.397(2)^\circ$ $b = 7.5121(8)$ Å, $\beta = 92.5850(10)^\circ$ $c = 22.658(2)$ Å, $\gamma = 90.2200(10)^\circ$
Volume/Å^3	1258.0(2)
Z, calculated density	2, 1.359 Mg/m^3
Absorption coefficient/mm^{-1}	1.294
F(000)	532
Crystal size/mm^3	$0.48 \times 0.42 \times 0.38$
Theta range for data collection	1.81° to 25.01°
Limiting indices	$-8 \le h \le 8$, $-8 \le k \le 8$, $-17 \le l \le 26$
Reflections collected/unique	6635/4353 [R(int) = 0.0680]
Completeness to theta = 25.01	98.5%
Absorption correction	semi-empirical from equivalents
Max. and min. transmission	0.6391 and 0.5755
Refinement method	full-matrix least-squares on F^2
Data/restraints/parameters	4353/1/224
Goodness-of-fit on F^2	0.977
Final R indices [$I > 2\sigma(I)$]	$R_1 = 0.0983$, $wR_2 = 0.2610$
R indices (all data)	$R_1 = 0.1409$, $wR_2 = 0.2942$
Largest diff. peak and hole	1.589 and –1.649 eÅ^3

Table 2. Selected bond lengths [Å] and bond angles [deg.] for $C_8Cd(s)$.[a]

Cl(5)–Cd(1)	2.64(2)	Cl(1)#1–Cl(5)–Cd(1)	88(6)
Cl(5)–Cd(2)#2	2.66(2)	Cl(1)#1–Cl(5)–Cd(2)#2	88(6)
Cd(1)–Cl(2)#1	2.519(4)	Cd(1)–Cl(5)–Cd(2)#2	175.7(11)
Cd(1)–Cl(2)	2.519(4)	Cl(2)#1–Cd(1)–Cl(2)	180.000(1)
Cd(1)–Cl(5)#1	2.64(2)	Cl(2)#1–Cd(1)–Cl(5)	84.4(6)
Cd(1)–Cl(3)	2.663(2)	Cl(2)–Cd(1)–Cl(5)	95.6(6)
Cd(1)–Cl(3)#1	2.663(2)	Cl(2)#1–Cd(1)–Cl(5)#1	95.6(6)
Cd(1)–Cl(1)#1	2.66(2)	Cl(2)–Cd(1)–Cl(5)#1	84.4(6)
Cd(1)–Cl(1)	2.66(2)	Cl(5)–Cd(1)–Cl(5)#1	180.000(7)
Cd(2)–Cl(4)	2.506(4)	Cl(2)#1–Cd(1)–Cl(3)	90.13(11)
Cd(2)–Cl(4)#3	2.506(4)	Cl(2)–Cd(1)–Cl(3)	89.87(11)
Cd(2)–Cl(3)#4	2.660(2)	Cl(5)–Cd(1)–Cl(3)	89.7(5)
Cd(2)–Cl(3)#5	2.660(2)	Cl(5)#1–Cd(1)–Cl(3)	90.3(5)
Cd(2)–Cl(5)#6	2.66(2)	Cl(2)#1–Cd(1)–Cl(3)#1	89.87(11)
Cd(2)–Cl(5)#1	2.66(2)	Cl(2)–Cd(1)–Cl(3)#1	90.13(11)
Cd(2)–Cl(1)#3	2.68(2)	Cl(5)–Cd(1)–Cl(3)#1	90.3(5)
Cd(2)–Cl(1)	2.68(2)	Cl(5)#1–Cd(1)–Cl(3)#1	89.7(5)
Cl(1)–Cl(5)#1	0.44(6)	Cl(3)–Cd(1)–Cl(3)#1	180.0
Cl(3)–Cd(2)#7	2.660(2)	Cl(2)#1–Cd(1)–Cl(1)#1	93.9(6)

[a]Symmetry codes: #1 $[-x+1, -y+1, -z+1]$; #2 $[x+1, y-1, z]$; #3 $[-x, -y+2, -z+1]$; #4 $[-x, -y+1, -z+1]$; #5 $[x, y+1, z]$; #6 $[x-1, y+1, z]$; #7 $[x, y-1, z]$.

Table 3. Hydrogen bond lengths (Å) and bond angles (deg) for $C_8Cd(s)$.[b]

D–H···A	d(D–H)	d(H···A)	d(D···A)	<DHA
N(1)–H(1A)···Cl(1)#1	0.89	2.46	3.25(3)	149.6
N(2)–H(2A)···Cl(3)#1	0.89	2.91	3.324(14)	151.9
N(2)–H(2B)···Cl(5)#1	0.89	2.82	3.54(3)	138.8
N(1)–H(1A)···Cl(5)	0.89	2.75	3.52(3)	145.7
N(1)–H(1A)···Cl(2)	0.89	2.91	3.531(16)	128.2
N(1)–H(1B)···Cl(5)#8	0.89	2.67	3.32(3)	130.8
N(1)–H(1B)···Cl(3)#9	0.89	2.72	3.450(15)	139.7
N(1)–H(1B)···Cl(1)#9	0.89	2.95	3.62(3)	133.4
N(1)–H(1C)···Cl(4)#10	0.89	2.41	3.280(14)	166.6
N(2)–H(2C)···Cl(2)#10	0.89	2.38	3.268(13)	176.9
N(2)–H(2A)···Cl(5)#5	0.89	2.84	3.35(3)	117.7
N(2)–H(2B)···Cl(1)	0.89	2.55	3.28(3)	139.8
N(2)–H(2B)···Cl(4)	0.89	2.79	3.481(15)	135.0

[b]Symmetry codes: #1 $[-x+1,-y+1,-z+1]$; #5 $[x,y+1,z]$; #8 $[-x+2,-y+1,-z+1]$; #9 $[x+1,y,z]$; #10 $[-x+1,-y+2,-z+1]$.

The crystallographic independent unit of the complex ($C_8Cd(s)$) is composed of two kinds of nonequivalent alkylammonium chains and one $[CdCl_4]^{2-}$ (see Fig. 1(a)), and the two different monomers of $[n\text{-}C_nH_{2n+1}NH_3]^+$ of the same complex (n-$C_nH_{2n+1}NH_3)_2CdCl_4$ are equal in the chemical composition way. From Fig. 1(b) and Table 2, we can see that the central ion (Cd^{2+}) adopts the six-coordinated configuration, an octahedral geometry is formed, and an infinite net is formed by $[CdCl_4]_n^{2n-}$. Figure 1(b) is drawn by means of ellipsoid, which can fully explain thermal effect of the carbon atoms in alkylammonium chains.

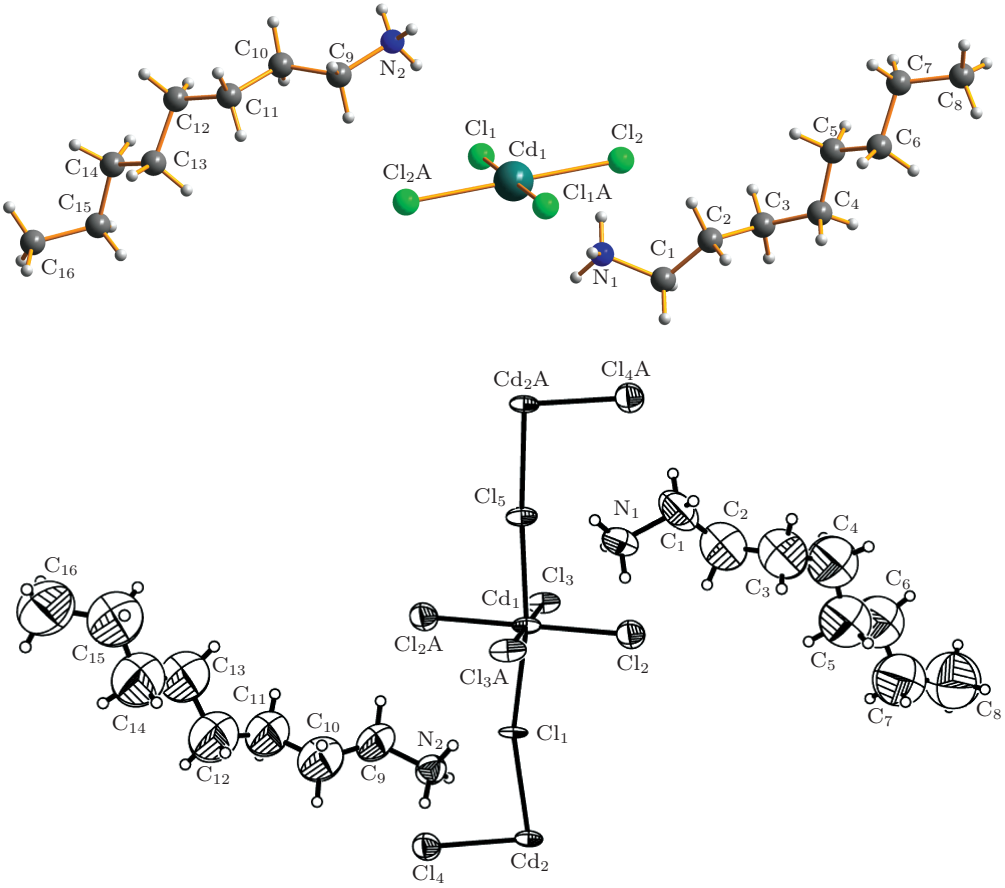


Fig. 1. (colour online) Molecular structure in a crystallographic independent unit of the complex $C_8Cd(s)$.

It is seen from Fig. 2 that the monomeric $[CdCl_4]_n^{2n-}$ moieties bind with the monomeric $[n\text{-}C_nH_{2n+1}NH_3]^+$ through several hydrogen bonds (see Table 3) when the crystal structure of ($C_8Cd(s)$) is viewed along the b axis. The classical N–H$\cdots$Cl hydrogen bonds are included in the complex ($C_8Cd(s)$). For the complex ($C_8Cd(s)$), the symmetric unit is stacked and a sandwich construction is formed, and the unit $[CdCl_4]_n^{2n-}$ resides in "sandwich floor", an infinite two-dimensional plane along the bc-plane is formed, and on account of binding action of hydrogen bonds, the molecule unit is extended to a space supermolecule, which helps to establish a two-dimensional perovskite structure. The results indicate that the hydrogen bonds play an important role in the stabilization of the whole structure. The steric configuration of the complex ($C_8Cd(s)$) is similar to other complexes $(n\text{-}C_nH_{2n+1}NH_3)_2MCl_4(s)$.

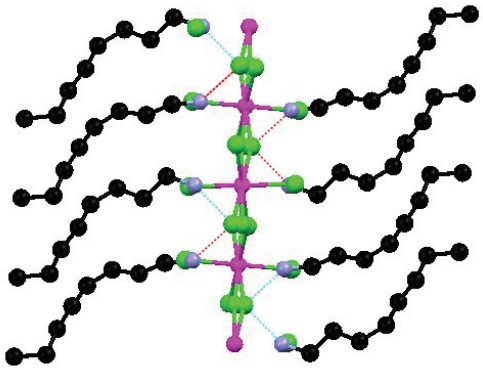


Fig. 2. (colour online) Packing structure of the complex $C_8Cd(s)$. Dashed lines represent the hydrogen bonds. Hydrogen atoms are omitted for clarity.

3.2. Lattice potential energy of the complex

Equation (1) is used to estimate the lattice potential energy for the general type of the salts M_pX_q:

$$U_{\rm POT} = |z_+|\,|z_-|\,v(\alpha'/V_{\rm m}^{1/3} + \beta'), \qquad (1)$$

where z_+ and z_- are the respective charges on the cation and anion of the complex, v is the number of ions per molecule and is equal to $(p+q)$. For the case of salt M_2X with charge ratio (1:2) such as ($C_8Cd(s)$), $z_+ = 1$, $z_- = 2$, $p = 2$, $q = 1$, $v = 3$, $\alpha' = 165.3$ kJ·mol^{-1}·nm, $\beta' = -29.8$ kJ·mol^{-1}, and $V_{\rm m}$ is in units of nm^3 and expressed as[18]

$$V_{\rm m}({\rm nm}^3) = M_{\rm m}/\rho N_{\rm A} = 1.66045 \times 10^{-3} M_{\rm m}/\rho, \quad (2)$$

where $N_{\rm A}$ is Avogadro's constant, and is 6.02245×10^{23} molecule·mol^{-1}. Thus, formula (1) is changed into[19]

$$U_{\rm POT} = \gamma(\rho/M_{\rm m})^{1/3} + \delta, \qquad (3)$$

where the values of the constants for M_2X (1:2) are: $\gamma = 8375.6$ kJ·mol^{-1}·cm and $\delta = -178.8$ kJ·mol^{-1}.[19] The density ρ (g·cm^{-3}) and molar mass $M_{\rm m}$ (g·mol^{-1}) are obtained from crystal structure data of the title complex in Table 1, $\rho = 1.359$ g·cm^{-3} and $M_{\rm m} = 514.70$ g·mol^{-1}, respectively. $V_{\rm m}$ is calculated to be 0.6289 nm^3 according to Eq. (2), consequently lattice potential energy of ($C_8Cd(s)$) is derived to be $U_{\rm POT} = 978.83$ kJ·mol^{-1}.

3.3. Low-temperature heat capacity

The experimental results of low-temperature heat capacities are plotted in Fig. 3.

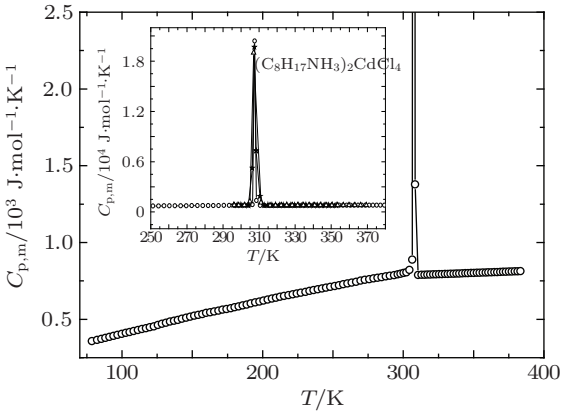


Fig. 3. (colour online) Curve of experimental molar heat capacities for the complex $C_8Cd(s)$. ("◯", "△" and "⋆" denote the first, second, and third series of measurements, respectively.)

In Fig. 3, only one obvious endothermic peak appears in a temperature range between 303 K and 310 K for ($C_8Cd(s)$). The experimental heat capacity values in temperature ranges between 78 K and 303 K and between 310 K and 384 K are, respectively, fitted by means of the least-square method, and two polynomial equations of experimental molar heat capacities ($C^{\rm o}_{\rm p,m}$) versus reduced temperature (X), $X = f(T)$, are obtained as follows.

Before the phase transition from 78 K to 303 K,

$$C^{\rm o}_{\rm p,m}\ ({\rm J\cdot K^{-1}\cdot mol^{-1}}) = 601.601 + 226.375X - 22.339X^2 - 0.944X^3; \quad (4)$$

After the phase transition from 310 K to 384 K,

$$C^{\rm o}_{\rm p,m}\ ({\rm J\cdot K^{-1}\cdot mol^{-1}}) = 800.877 + 12.839X - 0.782X^2 - 0.496X^3 + 1.094X^4, \qquad (5)$$

in which X is the reduced temperature, $X = [T - (T_{\max} + T_{\min})/2]/[(T_{\max} - T_{\min})/2]$ with T being the experimental temperature, $T_{\max}$ and $T_{\min}$ are the upper and lower limits in the temperature regions from 78 K to 303 K and 310 K to 384 K. The correlation coefficients of the fitting R^2 equal 0.99988 and 0.99991, corresponding to Eqs. (4) and (5).

3.4. Molar enthalpy and entropy of solid–solid phase transition

Three series of repeated heat capacity experiments in the phase transition region with different cooling rates for the sample are carried out so that the reversibility and repeatability of the phase transition of the sample are verified. The cooling rate of series 1 is about 15 K·min^{-1} (liquid nitrogen as the cooling agent), that of the series 2 is about 2.5 K·min^{-1} (ice-water cooling), and that of the series 3 is about 0.5 K·min^{-1} (natural cooling). The results of three series of repeated measurements are plotted in the inset of Fig. 3. It can be seen from the inset that there are some slight differences in the height and width of the peak between series of heat-capacity measurements during phase transitions of the sample. However, the phase transition basically exhibits good reversibility and repeatability, and different cooling rates do not affect the experimental results. The $C^{\rm o}_{\rm p,m}$ values of series of repeated experiments are in good agreement. The molar enthalpy of the phase transition ($\Delta_{\rm trs}H_{\rm m}$) in $C^{\rm o}_{\rm p,m}$–T curve is obtained from Eq. (6). The molar entropy $\Delta_{\rm trs}S_{\rm m}$ of the phase transition is calculated with the following thermodynamic Eq. (7):[20]

$$\Delta_{\rm trs}H_{\rm m} = \left[Q - n\cdot\int_{T_{\rm i}}^{T_{\rm trs}} C^{\rm o}_{\rm p(i)}\,{\rm d}T - n\cdot\int_{T_{\rm trs}}^{T_{\rm f}} C^{\rm o}_{\rm p(f)}\,{\rm d}T - \int_{T_{\rm i}}^{T_{\rm f}} H_0\,{\rm d}T\right]\Big/ n\ {\rm kJ\cdot mol^{-1}} \quad (6)$$

as

$$\Delta_{\rm trs}S_{\rm m} = \Delta_{\rm trs}H_{\rm m}/T_{\rm trs}\ {\rm J\cdot K\cdot mol^{-1}}, \quad (7)$$

where $T_{\rm i}$ in Eq. (6) the temperature is slightly smaller than the starting phase transition temperature; $T_{\rm f}$ is the temperature that is slightly higher than the finishing phase transition temperature; $C^{\rm o}_{\rm p,m(i)}$ is the heat capacity at temperature $T_{\rm i}$; $C^{\rm o}_{\rm p,m(f)}$ is the heat capacity at temperature $T_{\rm f}$; Q is the total heat quantity introduced to the calorimeter from temperature $T_{\rm i}$ to $T_{\rm f}$; $T_{\rm trs}$ is the peak temperature of the phase transition of the sample; n is the mole number of the sample; H_0 is the heat capacity of the empty sample cell. The values of Q and H_0 are calculated with the program stored in the computer linked with the adiabatic calorimetric system, and printed along with the experimental results of the heat capacities. The results of $T_{\rm trs}$ (K), $\Delta_{\rm trs}H_{\rm m}$ (kJ·mol^{-1}), $\Delta_{\rm trs}S_{\rm m}$ (J·K^{-1}·mol^{-1}), and their average values obtained from every series of repeated experiment are listed in Table 4.

Table 4. Results of the phase transitions obtained from three series of repeated experiments of $C_8Cd(s)$.

Thermodynamic properties	Series 1 x_i	Series 2 x_i	Series 3 x_i	Mean value[a] ($\bar{x} \pm \sigma_{\rm a}$)
$T_{\rm trs,1}$/K	307.51	307.01	307.42	(307.3 ± 0.15)
$\Delta_{\rm trs}H_{\rm m,1}$/(kJ/mol)	10.24	10.51	9.714	(10.15 ± 0.23)
$\Delta_{\rm trs}S_{\rm m,1}$/(J/K mol)	33.30	34.25	31.60	(33.05 ± 0.78)

[a] $\bar{x}$ is the mean value of a set of measurement results; $\sigma_{\rm a} = \sqrt{\sum_{i=1}^{n}(x_{\rm i} - \bar{x})^2/[n(n-1)]}$, n is the experimental number; x_i, a single value in a set of measurements.

For the title complex ($C_8Cd(s)$), there is a big phase change, which begins at about 303 K. The mechanism of the phase transition may be analogous to other complexes (n-$C_nH_{2n+1}NH_3)_2MX_4$.[21–24] With the increase of the temperature, the hydrogen bonds become weakened, which makes constraints between alkylammonium chains and $[CdCl_4]^{2-}$ become weakened. The partial disorder of alkylammonium chains occurs together with the reversal of polar NH_3 groups, thus the structure of the molecule is transformed, and another kind of free and partly disordered solid phase is formed, and leads to a dynamic order–disorder transition of rigid alkyl chains at the beginning, then, further conformational changes of the hydrocarbon part are dominant, complete disorder of the conformation is assumed to be similar to a "molten" state. When the phase transition is over, the whole solid phase is fully in disorder. After that, the whole solid–solid phase change finishes, and the complex holds the stable structure of new solid phase until solid–liquid

phase change occurs. Further research will continue to check the reasonableness of the analogy with the help of the variable temperature FTIR spectroscopy.

3.5. Smoothed heat capacities and thermodynamic functions of the complex

The smoothed molar heat capacities and thermodynamic functions are calculated based on the fitted polynomial equations of the heat capacities, each as a function of reduced temperature (X) according to the following thermodynamic equations:[25]

$$H_T^{\circ} - H_{298.15}^{\circ} = \int_{298.15}^{T} C_{\mathrm{p,m}}^{\circ} \mathrm{d}T, \tag{8}$$

$$S_T^{\circ} - S_{298.15}^{\circ} = \int_{298.15}^{T} \frac{C_{\mathrm{p,m}}^{\circ}}{T}\ \mathrm{d}T. \tag{9}$$

The polynomial fitted values of the molar heat capacities and fundamental thermodynamic functions of the sample relative to the standard reference temperature 298.15 K can be calculated at intervals of 5 K.

3.6. Thermodynamic properties of the complex

The thermodynamic properties of the complex according to the experimental data are described as follows.

Firstly, the lattice potential energy $U_{\mathrm{POT}}(\mathrm{C_8Cd}(s)) = 978.83\ \mathrm{kJ{\cdot}mol^{-1}}$. The result indicates that a strong electrostatic attraction exists between $[\mathrm{C_8H_{17}NH_3}]^+$ and $[\mathrm{CdCl_4}]^{2-}$ in the ($\mathrm{C_8Cd}(s)$). The value of lattice potential energy (LPE) shows that the structure of ($\mathrm{C_8Cd}(s)$) is very stable from the viewpoint of energy. Secondly, from Table 4 and Fig. 3, we can see that molar heat capacity of the ($\mathrm{C_8Cd}(s)$) is bigger, which shows that the strong intermolecular acting force exists in ($\mathrm{C_8Cd}(s)$), this may be caused by the high symmetry in the molecule ($\mathrm{C_8Cd}(s)$). Finally, from Table 4, $T_{\mathrm{trs}}(\mathrm{C_8Cd}(s))$ is 307.3 K (34.15 °C), which is lower. It indicates that the complex $\mathrm{C_8Cd}(s)$ is suitable for practical applications of phase-change energy storage. The molar enthalpy and entropy of the phase transition of ($\mathrm{C_8Cd}(s)$) are lower, this may be ascribed to an additional number of (–$\mathrm{CH_2}$–) groups adding into the cation and the enhancement of the steric hindrance, which results in decreases of enthalpy and entropy in the solid–solid phase transition.[25] According to Fig. 3, it is suggested that the solid-to-solid phase change is an order–disorder transition process.

Compared with a similar complex $(\mathrm{C_{12}H_{25}NH_3})_2\mathrm{ZnCl_4}(s)$[19] reported previously, the molar enthalpy and entropy of $(\mathrm{C_8H_{17}NH_3})_2\mathrm{CdCl_4}(s)$ are smaller than those of $(\mathrm{C_{12}H_{25}NH_3})_2\mathrm{CdCl_4}(s)$, but $T_{\mathrm{trs}}(\mathrm{C_{12}H_{25}NH_3})_2\mathrm{ZnCl_4}(s)$ is larger than $T_{\mathrm{trs}}(\mathrm{C_8H_{17}NH_3})_2\mathrm{ZnCl_4}(s)$. It may be attributed to the different metallic ions and cation radii of $[\mathrm{C_8H_{17}NH_3}]^+$ and $[\mathrm{C_{12}H_{25}NH_3}]^+$ existing in the two complexes. Lower or close to room temperature phase transition temperature is one of many measurement criterions determining whether a kind of phase transition material is useful in practical application in daily life. Consequently, based on the lower phase change temperature and larger phase transition enthalpy of the title complex, the complex ($\mathrm{C_8Cd}(s)$) is relatively appropriate for practical applications in the utilization of green energy. It can play an important role in effective utilization and storage of solar energy in future.

4. Conclusion

In this article, we mainly report on the crystal structure, lattice potential energy, and low temperature heat capacities of the crystalline complex ($\mathrm{C_8Cd}(s)$) in a temperature range from 78 K to 384 K. An obvious solid-to-solid phase transition is found in the $C_{\mathrm{p,m}}^{\circ}$–T curves. The temperature, molar enthalpy, and entropy of the solid–solid phase change are obtained. The relevant thermodynamic properties of the title complex are determined. The crystalline complex ($\mathrm{C_8Cd}(s)$), as a kind of phase change material, has significant applications in effective storage and utilization of solar energy. As is well known, a solar energy water heater cannot produce hot water without sunshine, while the phase-change materials of ($\mathrm{C_8Cd}(s)$) can be applied to a solar energy water heater to keep hot water at phase transition temperature for a long time. In addition, because the phase transition starting temperature (303 K) of ($\mathrm{C_8Cd}(s)$) is close to room temperature, it can be used for floor heating, which is good for human health.

References

[1] Maruoka N and Akiyama T 2003 *J. Chem. Eng. Jpn.* **36** 794

[2] Lu D F, Di Y Y and He D H 2011 *Acta Phys. Chim. Sin.* **27** 1319

[3] Liu Y P, Di Y Y, Dan W Y and He D H *J. Therm. Anal. Calorim.* DOI 10.1007/s10973-011-1737-9
[4] Hawes D W, Banu D and Feldman D 1990 *Solar Energy Mater.* **21** 61
[5] Lee K W, Lee C E, Kim J and Kang J K 2002 *Solid State Commun.* **124** 185
[6] Liu Y P, Di Y Y, Dan W Y, He D H, Kong Y X and Yang W W 2011 *Chin. Phys.* B **20** 028202
[7] Kang J K, Choy J H and Madeleine R L 1993 *J. Phys. Chem. Solids* **54** 1567
[8] Li W P, Zhang D S, Zhang T P, Wang T Z, Ruan D S, Xing D Q and Li H B 1999 *Thermochim. Acta* **326** 183
[9] Wu K Z, Zhang J J and Liu X D 2009 *Thermochim. Acta* **483** 55
[10] Arend H and Huber W 1978 *J. Cryst. Growth* **43** 213
[11] Tan Z C, Shi Q, Liu B P and Zhang H T 2008 *J. Therm. Anal. Calorim.* **92** 367
[12] White M A 1984 *Thermochim. Acta* **74** 55
[13] Di Y Y, Kong Y X, Yang W W and Tan Z C 2008 *Chin. Phys.* B **17** 3276
[14] Yang W W, Di Y Y, Kong Y X and Tan Z C 2010 *Chin. Phys.* B **19** 060517
[15] Sheldrick G M 2008 *Acta Cryst.* A **64** 112
[16] Tan Z C, Liu B P, Yan J B and Sun L X 2003 *J. Comput. Appl. Chem.* **20** 264
[17] Ditmars D A, Ishiha S, Chang S S and Bernstein G 1982 *J. Res. Natl. Bur. Stand.* **87** 159
[18] Jenkins H D B and Glasser L 2002 *Inorg. Chem.* **41** 4378
[19] Kong Y X, Di Y Y, Yang W W, Lü Y F and Tan Z C 2010 *Chin. J. Chem.* **28** 521
[20] Di Y Y, Tan Z C, Wu X M, Meng S H and Qu S S 2000 *Thermochim. Acta* **356** 143
[21] Lee C H, Lee K W and Lee C E 2003 *Curr. Appl. Phys.* **3** 477
[22] Guo N and Wang W 1994 *Chin. J. Appl. Chem.* **11** 25 (in Chinese)
[23] Zuo P, Wu K Z, Cui W Z and Liu X D 2002 *J. Hebei Norm. Univ.* (Natural Science Edition) **26** 53 (in Chinese)
[24] Guo N, Wang W, Zeng G F and Xi S Q 1994 *Acta Chim. Sin.* **52** 705 (in Chinese)
[25] Tong B, Liu Q S, Tan Z C and Welz-Biermann U 2010 *J. Phys. Chem.* A **114** 3782